Control of morphology and nucleation density of iron oxide nanostructures by electric conditions on iron surfaces exposed to reactive oxygen plasmas

U. Cvelbar,[1,a] K. Ostrikov,[2,3] I. Levchenko,[2,3] M. Mozetic,[1] and M. K. Sunkara[4]
[1]*Jozef Stefan Institute, Jamova cesta 39, SI-1000 Ljubljana, Slovenia*
[2]*Plasma Nanoscience Centre Australia (PNCA), CSIRO Materials Science and Engineering, P.O. Box 218, Lindfield, New South Wales 2070, Australia*
[3]*Plasma Nanoscience, School of Physics, University of Sydney, Sydney, New South Wales 2006, Australia*
[4]*Department of Chemical Engineering, University of Louisville, Louisville, Kentucky 40292, USA*

(Received 28 April 2009; accepted 8 May 2009; published online 29 May 2009)

The possibility to control the morphology and nucleation density of quasi-one-dimensional, single-crystalline α-Fe_2O_3 nanostructures by varying the electric potential of iron surfaces exposed to reactive oxygen plasmas is demonstrated experimentally. A systematic increase in the oxygen ion flux through rf biasing of otherwise floating substrates and then an additional increase of the ion/neutral density resulted in remarkable structural transformations of straight nanoneedles into nanowires with controlled tapering/aspect ratio and also in larger nucleation densities. Multiscale numerical simulations relate the microscopic ion flux topographies to the nanostructure nucleation and morphological evolution. This approach is applicable to other metal-oxide nanostructures. © *2009 American Institute of Physics*. [DOI: 10.1063/1.3147193]

The ability to control the nucleation, morphological, and other properties of nanostructures (NSs) and their arrays by optimizing the process conditions that is essential for the development of next-generation nanotechnologies, still remains limited despite two decades of research.[1–4] Low-temperature plasmas offer a broad range of possibilities to control the shape, size, and properties of a very large number of nanoscale systems.[5–8] One of the peculiar features of this environment are the ion and electron currents onto the surface, which can be connected or disconnected from the biasing circuits. In the former case, the substrate is under the floating potential and the electron and ion currents balance each other so that the associated heating is limited to only a few topmost atomic layers. If the substrate is conducting and is connected to the circuit, the net current can flow through it causing significant heating throughout the substrate.[9] This may create additional possibilities to tailor NSs on surfaces, yet this possibility still remains unexplored. Here we show that by controlling the potential difference (and hence the electron/ion fluxes onto the substrate) between the plasma and the substrate, one can control the morphology and density of nucleation of quasi-one-dimensional (quasi-1D), single-crystalline α-Fe_2O_3 NSs. The experimental and numerical results suggest that stronger ion fluxes result in morphological transformations of straight nanoneedles (NNs) into slightly tapered nanowires, and also in higher NS densities unusual electrical and mechanical properties of these NSs make them promising for various applications.[10] Ultimate control of the NS sizes/shapes and nucleation densities can improve the performance of nanodevices and is of interest.[11,12]

The arrays of α-Fe_2O_3 NSs were synthesized by exposing Fe substrates to oxygen plasmas generated in a 27.12 MHz rf discharge sustained in the system sketched in Fig. 1. The reactor was made of Pyrex glass. The flanges were made of aluminum. The reactor was a cylindrical tube of 11 cm in diameter and 30 cm in length. The oxygen pressure range, the base pressure, and the maximum rf power were 75–150 Pa, 1 Pa, and 5 kW, respectively. Movable fiber optics catalytic and double Langmuir probes were used to measure a range of the plasma parameters, including the densities of neutral/ionic species and the electron temperature.[13,14] The probes were inserted through side ports as close as possible to the growth surface. The Langmuir probe was almost at the position of the sample, whereas the catalytic probes were inserted through the glass side arms in order to measure only diffusion-governed neutral atoms, the average surface temperature was measured by a IR camera. The samples used were iron foils of thickness 1.7 mm and cut to pieces of approximately 15 mm^2. The NSs were grown in the essentially catalyst-free mode. To additionally control the potential difference between the plasma and the sample surface, the sample could be either connected or disconnected from the rf circuit as shown in Fig. 1. The voltage was measured with a high-voltage electric probe, and the plasma-surface potential drop was calculated using the measured plasma parameters.[13,15] When the substrate holder was not connected to the rf generator, the sample was under the (low) floating potential; otherwise the samples were subjected to the sig-

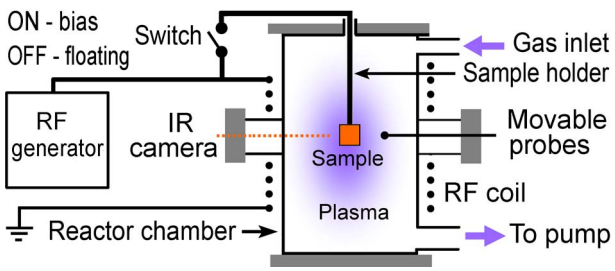

FIG. 1. (Color online) Schematic of the experimental setup with the rf plasma reactor for Fe_2O_3 NN/nanowire growth on iron substrates exposed to reactive oxygen plasmas.

[a]Electronic mail: uros.cvelbar@ijs.si.

TABLE I. Parameters of the experiment and the plasma.

Case	T_S (°C)	n_0 (m^{-3})	n_i (m^{-3})	T_e (eV)	Bias type	U_S (V)
(1)	585	1.7×10^{21}	4×10^{16}	4 ± 1	floating	−15
(2)	585	1.59×10^{21}	3×10^{16}	3.5 ± 1	rf–self-bias	−150
(3)	660	1.7×10^{21}	4×10^{16}	4 ± 1	rf–self-bias	−150

nificantly larger rf self-bias. The samples were analyzed by the scanning and transmission electron microscopy (SEM/TEM). Other details of the equipment, sample preparation and characterization can be found elsewhere.[16]

The three sets of the experimental parameters listed in Table I were selected to (i) produce the NSs just above and further away from the α-Fe_2O_3 phase transition temperature;[10,16] (ii) increase the ion flux from one set to another; (iii) maintain the average surface temperature the same in sets (1) and (2) by increasing the surface bias and simultaneously decreasing the neutral/ion densities; and (iv) study the effect of the increased surface temperature under the same electric conditions on the surface [sets (2) and (3)]. In Table I, T_s is the surface temperature, n_0 is the density of neutral atoms, n_i is the ion density, T_e is the electron temperature, and U_S is the surface-to-plasma potential difference. The shapes, sizes, and the nucleation densities in these three cases were different as can be seen in Figs. 2(a)–2(c). Straight NNs [Fig. 2(a)] developed under the floating potential conditions, whereas short [Fig. 2(b)] and long [Fig. 2(c)] tapered nanowires appeared when the sample was connected to the rf circuit. In all cases, the NSs were single-crystalline α-Fe_2O_3, and grew along the [110] crystallographic direction as confirmed by the bright-field [Fig. 2(d)] and high-resolution [Fig. 2(e)] TEM (HRTEM) images and the associated fast Fourier transform (FFT) patterns [Fig. 2(f)].

The dependence of the NN/nanowire length and surface density on the base diameter under the three sets of the process conditions are shown in Fig. 3. The NNs grown under the floating potential conditions are typically thin with a very small diameter variation between the base and the tip. Their mean length reaches 1000 nm. However, biasing the substrate [and maintaining T_s the same as in case (1)] results in larger base widths and a modest tapering of the NSs, which generally become slightly longer than the NNs. Thus, substantially larger U_S (at the same T_s) increases the mean diameter from 50 [case (1)] to 120 nm [case (2)] and the mean length of the NSs from 1100 [case (1)] to 1400 nm [case (2)] as can be seen in Fig. 3(a). With the increased bias, the integrated density of the NSs also increases despite a small decrease in the peak value [Fig. 3(b)]. When the surface temperature is increased from 585 to 660 °C at the same applied bias (−150 V), the average nanowire diameter increases even more from 120 [case (2)] to 150 nm [case (3)]. The average NS length increases even more significantly from 1400 [case (2)] to 2500 nm [case (3)] as can be seen in Fig. 3(a). The density of the nanowires on the surface also becomes larger [Fig. 3(b)]. Thus, increasing ion flux from case (1) to cases (2) and eventually (3) results in the morphological transition from straight and relatively thin nanocones to wider and much longer tapered nanowires. The surface density of the NSs also increases as the ion fluxes become stronger and the surface temperature increases.

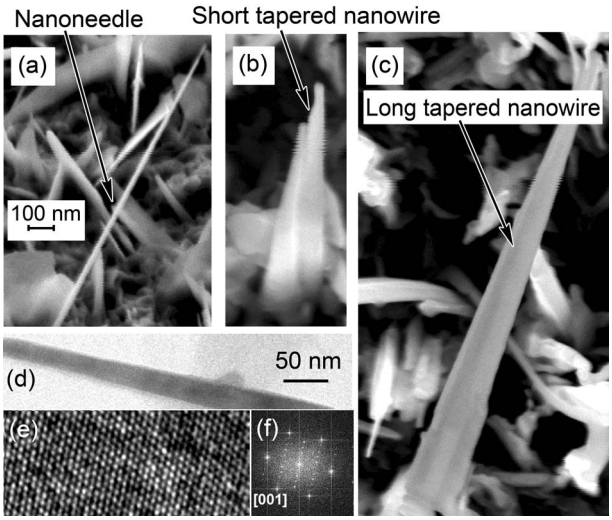

FIG. 2. (a) Typical Fe_2O_3 NNs, (b) short, and (c) long tapered nanowires grown on Fe substrates exposed to oxygen plasmas generated in the rf plasma reactor. (d) Bright-field TEM image of a NN. (e) HRTEM image showing the single-crystalline structure. (f) The corresponding FFT image.

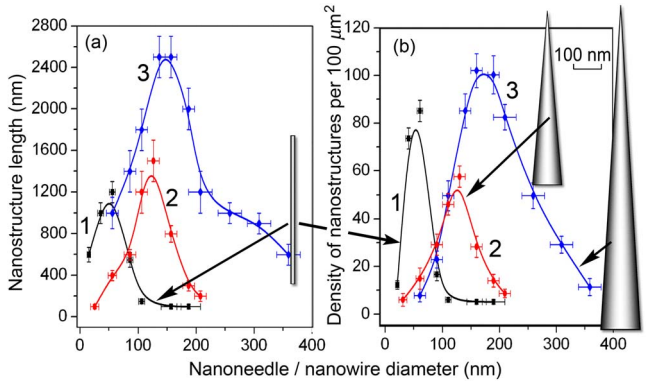

FIG. 3. (Color online) (a) Dependence of the length and (b) the surface density of NSs on the base diameter under the three sets of growth conditions of Table I. Typical NS shapes are drawn to the actual scale. The curves are labeled (1)–(3) according to Table I.

To explain the observed transformations, we performed a multiscale Monte-Carlo simulations of microscopic ion fluxes onto the NS and substrate, and invoked the vapor-solid-solid (VSS) mechanism, commonly used in nanowire growth from the supersaturated solid phase.[10,16,17] The model considers ion movement in the plasma-surface sheath and allows calculation of flux distribution on the NS and substrate surfaces. The details of the calculations are described elsewhere.[18] The results are shown in Fig. 4(a). The simulation results suggest that in case (1), the flux is concentrated near the NN tips and barely reaches the bases. In case (2), the flux is distributed uniformly over the nanowire surfaces and a significant fraction of the flux reaches their bases. In case (3), the ion flux is predominantly deposited near the bases. Putting these results in the context of the VSS nucleation and growth from size- and position-nonuniform morphology elements (nanohillocks) on the iron surface, one can conclude the following. In case (1), the NNs nucleate in relatively small "hot spots," where conditions for the nucleation of platelets of single-crystalline iron oxide NSs at the solid (supersaturated Fe)–vapor (oxygen plasma) interface are met. The size of these spots is determined by the surface temperature and is not affected by the ion fluxes and hence, does not change during the growth. This is why the NNs emerge,

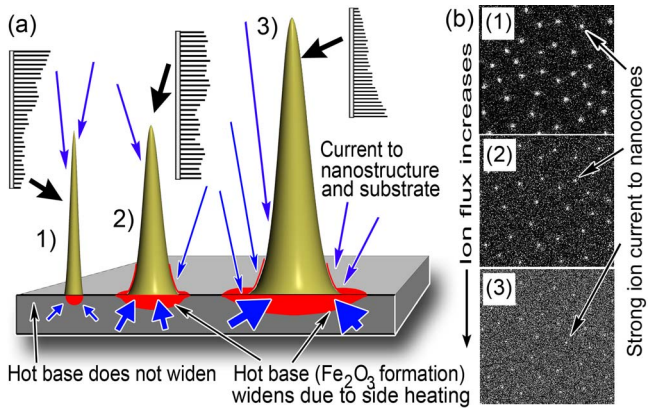

FIG. 4. (Color online) Scheme of Fe_2O_3 NN and nanowire growth on a Fe substrate by VSS mechanism in oxygen plasmas, and the ion flux distributions on lateral surfaces of NSs (a) and over the substrate surface (b) for three cases [(1)–(3)] listed in Table I, computed by the MC technique (Ref. 18). At low substrate bias [case (1)], the ion fluxes are focused on relatively sharp nanohillocks, the NS is formed with a small base diameter and develops as a NN without widening. At larger bias [case (2)], the ion flux increases and becomes more uniformly distributed over the NS and substrate surfaces. In case (3) when the surface temperature is increased, the ion flux is predominantly deposited near the nanowire bases, and the base diameter increases due to widening of the hot base.

platelet-by-platelet, without any significant diameter changes. In case (2), the sizes and local temperatures of the hot spots are affected by the ion fluxes. Localized heating creates larger nucleation areas, which increase during the growth as more and more ions deposit near the NS base; this explains the observed tapering. However, since the supply of oxygen atoms was reduced [compared to case (1)], the length increase was insignificant as can be seen in Fig. 3(a). An increase in the temperature in case (3) led to significantly larger nucleation spots, which increase with the temperature.[10] An increased supply of oxygen to the nucleation spots (both because of stronger ion fluxes more focused on the nanowire bases and of larger densities of oxygen atoms, see Table I) resulted in the growth of much longer nanowires [Fig. 3(a)]. The nucleation spots supersaturate and expand faster, hence, the bases of the nanowires are notably larger than in cases (1) and (2).

To interpret the effect of the systematically increasing ion fluxes on the NS nucleation density, we have computed and visualized the two-dimensional distribution of ion fluxes over the surface areas of 10 μm^2 shown in Fig. 4(b) that correspond to cases (1)–(3), respectively. The flux distribution around the NSs is represented by the gray-tone visualization with the lighter points corresponding to the stronger flux, and vice versa. These results suggest that the distribution of the ion fluxes (and the associated localized heating) is very nonuniform in case (1) (this is illustrated by light spots indicating the strong flux to the NSs), and becomes more and more uniform as the ion flux increases (in panel 3, the entire substrate is covered with the gray tint). Since at low U_S the ion fluxes are focused on relatively sharp nanohillocks[19] and the surface temperature is low, the NSs only nucleate in those "locally sharp" areas, whose density is relatively low. When the plasma-to-surface potential difference becomes larger, the flux increases and becomes more uniformly distributed over the surface [Fig. 4(b), inset 2]. Areas of impact of higher-energy ions create additional nucleation spots; this explains a larger NS density in case (2). When the ion flux increases even more and the temperature also increases [case (3)], conditions for nucleation are met on a larger number of nanohillocks, and more nucleation spots are created by the ion impact. We have also observed that if the samples are further heated to T_s=750 °C, the surface quickly becomes supersaturated and the film nucleation occurs over the entire surface area, and no NSs are formed. This further supports our model based on the temperature dependence of the hot spot size.

In summary, the treatment of iron surface with plasmas under the floating bias conditions leads to the growth of narrow (50 nm diameter) and long (1200 nm) single-crystalline α-Fe_2O_3 NNs, whereas the use of a −150 V bias resulted in the formation of tapered nanowires with the average base diameters of 200–300 nm and lengths up to 1500 nm at a surface temperature of 585 °C, and up to 2500 nm at T_s =660 °C. Multiscale numerical simulations have related the observed morphological transformations and the increasing NS nucleation density to the microscopic distributions of ion fluxes over the NN/nanowire and substrate surfaces. This approach is generic and can be used for deterministic synthesis of a broader range of single-crystalline metal oxide quasi-1D NSs on solid surfaces exposed to low-temperature nonequilibrium reactive plasmas.

[1]W. R. L. Lambrecht, C. H. Lee, B. Segall, J. C. Angus, Z. Li, and M. Sunkara, Nature (London) **364**, 607 (1993).
[2]M. Mozetic, U. Cvelbar, M. K. Sunkara, and S. Vaddiraju, Adv. Mater. (Weinheim, Ger.) **17**, 2138 (2005).
[3]K. Ostrikov, Rev. Mod. Phys. **77**, 489 (2005).
[4]M. Keidar, I. Levchenko, T. Arbel, M. Alexander, A. M. Waas, and K. Ostrikov, Appl. Phys. Lett. **92**, 043129 (2008).
[5]M. Keidar, O. R. Monteiro, A. Anders, and I. D. Boyd, Appl. Phys. Lett. **81**, 1183 (2002).
[6]U. Cvelbar, K. Ostrikov, A. Drenik, and M. Mozetic, Appl. Phys. Lett. **92**, 133505 (2008).
[7]R. M. Sankaran, D. Holunga, R. C. Flagan, and K. P. Giapis, Nano Lett. **5**, 537 (2005).
[8]I. Levchenko, K. Ostrikov, K. Diwan, K. Winkler, and D. Mariotti, Appl. Phys. Lett. **93**, 183102 (2008).
[9]D. Mariotti, V. Švrček, and D.-G. Kim, Appl. Phys. Lett. **91**, 183111 (2007).
[10]U. Cvelbar, Z. Chen, M. K. Sunkara, and M. Mozetic, Small **4**, 1610 (2008).
[11]X. Wu, X. X. Zhong, and K. Ostrikov, Appl. Phys. Lett. **92**, 223104 (2008).
[12]I. Levchenko, K. Ostrikov, J. D. Long, and S. Xu, Appl. Phys. Lett. **91**, 113115 (2007).
[13]M. Mozetic, A. Vesel, U. Cvelbar, and A. Ricard, Plasma Chem. Plasma Process. **26**, 103 (2006).
[14]K. N. Ostrikov, S. Xu and A. B. M. S. Azam, Plasma Phys. Controlled Fusion **35**, 531 (1993).
[15]Q. Cheng, S. Xu, J. Long, and K. Ostrikov, Appl. Phys. Lett. **90**, 173112 (2007).
[16]Z. Chen, U. Cvelbar, M. Mozetic, J. He, and M. K. Sunkara, Chem. Mater. **20**, 3224 (2008).
[17]J. Arbiol, B. Kalache, P. Roca i Cabarrocas, J. R. Morante, and A. Fontcuberta i Morral, Nanotechnology **18**, 305606 (2007).
[18]I. Levchenko and K. Ostrikov, J. Phys. D **40**, 2308 (2007).
[19]E. Tam, I. Levchenko, and K. Ostrikov, J. Appl. Phys. **100**, 036104 (2006).